Construction and Building Materials 346 (2022) 128440

Contents lists available at ScienceDirect

Construction and Building Materials

journal homepage: www.elsevier.com/locate/conbuildmat

Investigation of material characteristics and hygrothermal performances of different bio-based insulation composites

C.H. Koh *, F. Gauvin, K. Schollbach, H.J.H. Brouwers

Department of the Built Environment, Eindhoven University of Technology, P. O. Box 513, 5600 MB Eindhoven, the Netherlands

ARTICLE INFO

Keywords:
Bio-based insulation
Thermal conductivity
Moisture
Hygrothermal performance
Mould growth

ABSTRACT

The thermal and hygric characteristics of four bio-based insulation composites (mycelium, hemp, grass and cork) are investigated, and their hygrothermal performances including mould growth potential are simulated and analysed under typical construction details and various climates profiles. The cork composite is found to have the best hygrothermal performance and is suitable under all investigated climates without mould growth, due to its hydrophobic nature and low thermal conductivity. The mycelium composite is highly susceptible to mould growth risk; whereas medium risk is observed on both hemp and grass composites. The findings underline the suitability of using different bio-based composites according to the assembly design and the local climate conditions.

1. Introduction

The building construction industry accounted for 37 % of global energy-related greenhouse gas (GHG) emissions in 2020, 10 % of which resulted from the manufacturing of building construction materials [1]. Along with reducing energy demand and decarbonizing power supply, it is essential to address the embodied energy within the building materials and their manufacturing process for decarbonizing the global buildings and construction sector [2]. Policies on incorporating whole-life carbon have already gained traction in countries such as the Netherlands, Denmark and France where CO_2 limits are imposed on new buildings, and more countries are expected to have similar policies in place to achieve carbon neutrality as a whole [2].

Bio-based building materials, either wood-based or containing other natural fibres are one of the solutions for producing low carbon materials. They generally have a lower embodied energy than synthetic materials, can be sourced locally, and have diverse building applications to achieve the desired performance characteristics [3]. Plant-based materials such as hemp, expanded cork, straw, grass, etc. are particularly well suited for providing a satisfactory thermal insulation performance owing to their porous structure and consequently low thermal conductivity in the range of 0.037 and 0.080 $W{\cdot}m^{-1}{\cdot}K^{-1}$ [4]. However, the most frequently used thermal insulation materials in Europe are inorganic mineral fibres, e.g. glasswool and stone wool, follow by organic fossil fuel derived foams, e.g. expanded and extruded polystyrene and polyurethane, whilst all other materials only cover the remaining 1 % of the market [5], including plant-derived materials. A large potential saving on GHG emissions can be realized by popularising the usage of bio-based insulation materials.

The lack of widespread usage of bio-based insulation materials can be attributed to their intrinsic hygroscopic nature and tendency to absorb moisture from their surroundings [6], and the associated durability concerns such as mould development [7] under humid environments. Building component with the presence of organic matter is more susceptible to mould infestation than inorganic materials [8]. And with the growth of energy-efficient buildings which are relying on airtightness and highly insulate envelope design, these buildings are found to have higher indoor humidity, which consequently supports mould germination and growth [9]. Alarmingly, adverse health symptoms associated with exposure to indoor moulds, such as asthma, allergies and infections have been studied and established [9]. And the use of bio-based materials has provided the optimal medium for fungal proliferation in the built environment. In view of that, it is essential to study the hygroscopic properties and mould growth potential of bio-based insulation materials, coupled with their hygrothermal performance under different environmental conditions, to overcome these concerns and to provide a factual guideline for engineers and architects.

In this research, four bio-based insulation composites (cork, grass, hemp, and mycelium) are selected to examine their hygroscopic properties and hygrothermal performances under predefined built

* Corresponding author.
E-mail address: k.c.h.koh.chuen.hon@tue.nl (C.H. Koh).

https://doi.org/10.1016/j.conbuildmat.2022.128440
Received 31 May 2022; Received in revised form 5 July 2022; Accepted 8 July 2022

environments. These composites are selected based on their (i) low thermal conductivity, (ii) low embodied energy and preferrable composed of recycled or waste material, and (iii) commercially available. The declared thermal conductivity of these composites is around 0.040 $W{\cdot}m^{-1}{\cdot}K^{-1}$ [10–13], which is in the same range as other conventional building insulation materials [14]. Besides, their embodied energy is considered low, since they are made of either agriculture residues or recycled materials, and do not require an energy-intensive production process. An exception is made for mycelium composite whose production methods e.g. sterilization and inoculation [15] suggest a higher embodied energy than other bio-based materials, however, is included for its novelty as sustainable bio-based insulation material.

Several authors have investigated comparable insulation materials. A comprehensive hygrothermal characterization of expanded cork for building facades is provided by Simões et al. [16], where the studied cork boards are observed to have low thermal conductivity ranging from 0.037 to 0.041 $W{\cdot}m^{-1}{\cdot}K^{-1}$ with good resistance during long term durability testing. Relevant heat transfer modelling and hygrothermal simulations on the cork boards have also been carried out by the same research group [17,18] and provide valuable insights into heat and moisture transport phenomena under the simulated built environment. An overview of grass-based composites is presented in [19], showing average thermal conductivities between 0.034 and 0.09 $W{\cdot}m^{-1}{\cdot}K^{-1}$, and also highlighting their good sorption desorption capability. For hemp-based composite, Latif et al. [20] and Collet et al. [21] have reported that hemp wools show higher sorption and similar vapour resistance factor as mineral wools. The thermal conductivities of hemp wool are reported between 0.038 and 0.06 $W{\cdot}m^{-1}{\cdot}K^{-1}$ [4]. Different mycelium-based composites have also been developed by various research groups, e.g. mycelium-miscanthus composites by Dias et al. [22] with reported thermal conductivities between 0.0882 and 0.104 $W{\cdot}m^{-1}{\cdot}K^{-1}$; mycelium-flax, mycelium-hemp and mycelium-straw by Elsacker et al. [15] at 0.0578, 0.0404, 0.0419 $W{\cdot}m^{-1}{\cdot}K^{-1}$ respectively; and mycelium bio-foam by Yang et al. [23] from 0.05 to 0.07 $W{\cdot}m^{-1}{\cdot}K^{-1}$.

The hygrothermal models are widely used to simulate the coupled heat and moisture transport process for one or multidimensional cases, by either taking into account a single building component or a complete building envelope [24]. Material properties are first investigated in the lab and applied as inputs in the hygrothermal simulation tool, together with the other two main inputs, i.e. geometry of the enclosure and boundary conditions. By combining different boundary conditions (e.g. exterior and interior climate) and geometry (design of building components), the hygrothermal performance of different built environments can be simulated and predicted using validated software. In this paper, European cities representing different climate zones as per Köppen climate classification are selected for the exterior boundary conditions, and the enclosure geometry is modelled one-dimensionally based on typical assembly wall designs found in cold climate zones.

The durability and hygrothermal performance of innovative bio-based insulation materials has not been widely investigated and many open questions remain with regard to efficiency and resistance to mould growth. This comparative study aimed to verify the performance of commercially available and state-of-the-art bio-based insulation material, and to aid in the optimal selection and application of these materials under different conditions. The thermal and hygric characteristics of the selected materials are examined and used to simulate their hygrothermal performance under different construction details and various climates in Europe. Mould growth potential is further simulated and compared against laboratory results, to better assess the durability and fungal resistance of these bio-based insulation materials.

2. Material and methodology

The material properties and hygrothermal performance of the selected bio-based insulation material are evaluated using the methodology shown in Fig. 1. Hygrothermal material properties and mould growth potential are measured in the lab, while the software is used to model and simulate the performance of wall assemblies containing the investigated bio-based insulation composites under different boundary conditions.

2.1. Material

The chosen bio-based insulation composites are shown in Fig. 2: (a) mycelium composite made of locally sourced agricultural biomass like straw, miscanthus and flax with the mycelium growing on them and acting as a binder, produced and supplied by Fairm [12]; (b) grass composite made of 72 % fibres extracted from grass clippings, 20 % jute fibres from recycled cocoa and coffee sacks, and 8 % polyester binder fibres, bound through airlaying and thermobonding process, produced and supplied by Gramitherm [10]; (c) hemp composite made of 66 % fibres from industrial hemp plant, 22 % jute fibres from recycled cocoa and coffee sacks, 8 % polymeric support fibres based on recycled PET, and 4 % soda, produced and supplied by HempFlax [11]; and (d) cork composite made of expanded cork by autoclaving and steam-baking blond cork granules at 350 °C, and the product is formed and bound with its natural resin (suberin) during the heating process, produced by Amorim PT and supplied by Pro Suber [13].

2.2. Material properties characterization

2.2.1. Density and porosity

The total porosity of the samples (open and closed pores) are calculated from their particle density $\rho_{particle}$ ($kg{\cdot}m^{-3}$) and bulk density ρ_{bulk} ($kg{\cdot}m^{-3}$) by.

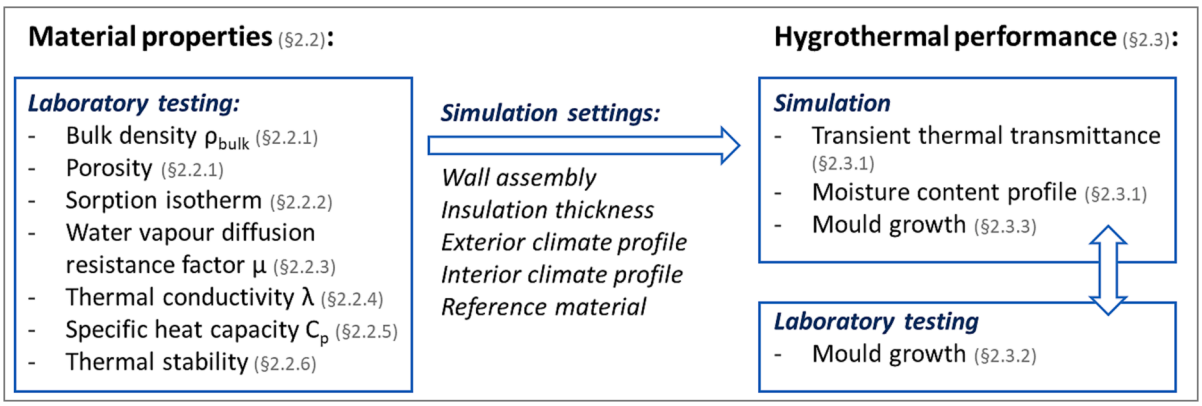

Fig. 1. Methodology overview.

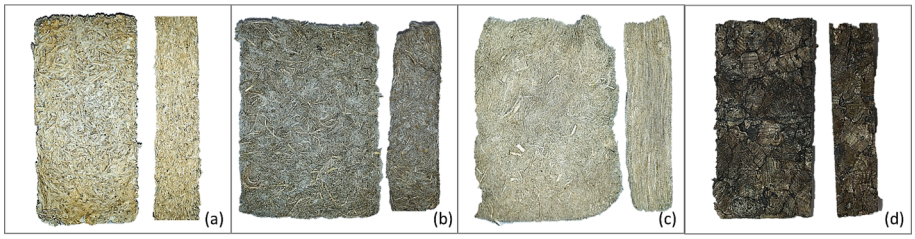

Fig. 2. (a) mycelium, (b) grass, (c) hemp, (d) cork composites.

$$porosity = 1 - \frac{\rho_{bulk}}{\rho_{particle}} \quad (1)$$

Helium pycnometer (Micromeritics AccuPyc II 1340) is used to measure their $\rho_{particle}$.

2.2.2. Sorption isotherm

The sorption isotherms of insulation materials are obtained by means of conditioning under aqueous solutions [25]. The samples are first dried in an oven at 50 °C until the constant mass is achieved to attain their dry weight m_{dry}. The dry samples are then conditioned in desiccators containing different saturated salt solutions with a constant relative humidity RH, i.e. magnesium chloride hexahydrate $MgCl_2{\cdot}6H_20$ for 33 % RH, potassium carbonate K_2CO_3 for 43 % RH, sodium bromide NaBr for 59 % RH, sodium chloride NaCl for 75 % RH, potassium chloride KCl for 85 % RH, and potassium sulfate K_2SO_4 for 98 % RH. The desiccators are kept in a climatized room with a constant temperature of 20 °C. The weighing is done in 24-hour intervals, and if 5 successive weighings show a mass loss change of less than 0.1 %, it is assumed that constant mass m is achieved. For desorption, the same samples are transferred from a higher RH desiccator to a lower RH desiccator, and their equilibrium masses are to be measured with the same procedure. The equilibrium moisture contents w ($\%kg^3{\cdot}kg^{-3}$) are plotted against relative humidity RH (%) for both sorption and desorption curves.

Free water saturation w_{sat} is approximated by conditioning the specimen at 100 % RH by fully immersing the specimen in water for 7 days at room temperature. The surface of samples is then lightly blotted with a damped sponge to remove excess water and their weight is measured.

2.2.3. Water vapour diffusion resistance factor

The water vapour diffusion resistance factor μ is measured using both the wet cup (water) method and the dry cup (desiccant) method according to standard ASTM E96 [26]. The cups are filled with anhydrous calcium chloride $CaCl_2$ for the dry cup method and distilled water for the wet cup method. Specimen with a thickness d_μ (m) are attached to the cups with a specific exposed area A_μ (m^2) and the edges are sealed to block vapour passage at the edge of the specimen. The test cups are kept in a climatized room at 60 % RH and 20 °C. The change of mass Δm (kg) at successive times Δt (s) is measured by weighing the cups to obtain the density of water vapour transmission rate g ($kg{\cdot}m^{-2}{\cdot}s^{-1}$) as.

$$g = \frac{1}{A_\mu}\frac{\Delta m}{\Delta t} \quad (2)$$

The measurement is considered complete once five successive values of g only vary within ± 5 %. The value of μ (dimensionless) is then calculated using.

$$\mu = \frac{\Delta p{\cdot}\delta_{air}}{g{\cdot}d_\mu} \quad (3)$$

where Δp (Pa) is water vapour partial pressure difference and δ_{air} ($kg{\cdot}m^{-1}{\cdot}s^{-1}{\cdot}Pa^{-1}$) is the water vapour permeability of air.

2.2.4. Thermal conductivity

The transient line source method is utilized for the measurement of thermal conductivity λ ($W{\cdot}m^{-1}{\cdot}K^{-1}$) by using a thermal needle probe (AP Isomet model 2104), with a declared accuracy of 5 % of the reading plus 0.001 $W{\cdot}m^{-1}{\cdot}K^{-1}$. Samples under three RH conditions (0 %, 50 % and 80 %) are examined for their λ values. The samples are dried at 50 °C in an oven (Memmert universal oven UF260) to reach near 0 % RH and conditioned in a climate chamber (Memmert climate chamber ICH750) for 50 % and 80 % RH, all until constant weight is achieved. The samples are protected using low vapour permeability plastic wrap before and during the λ measurements to maintain their moisture content. The λ measurements are taken at room temperature (20 ± 2 °C).

2.2.5. Specific heat capacity

For specific heat capacity C_p ($J{\cdot}kg^{-1}{\cdot}{}^{\circ}C^{-1}$), differential scanning calorimetry DSC (TA Instruments DSC Q2000) is used at temperatures from −20 °C to 50 °C at a heating/cooling ramp of 10 $°C{\cdot}min^{-1}$ in a nitrogen atmosphere with a flow of 50 $ml{\cdot}min^{-1}$. Three heat-cool cycles are run for each sample, and C_p value at 20 °C from the third heat cycle is taken for subsequent hygrothermal study. 5–10 mg of crushed samples are prepared for mycelium, hemp and grass composites, and 3–5 mg for cork composite.

2.2.6. Thermal stability

Thermogravimetric analyser TGA (TA Instruments TGA Q500) is further used to investigate the thermal stability of samples from room temperature up to 650 °C at a heating rate of 5 $°C{\cdot}min^{-1}$ in a nitrogen atmosphere with a flow of 60 $ml{\cdot}min^{-1}$ by observing their mass change due to thermal degradation.

2.3. Hygrothermal performances assessment

Heat, air and moisture transport (HAM) simulations are performed for two different wall assemblies exposed in six exterior climates, while the indoor climate remains the same. The annual moisture content of the insulation materials is analysed, with a special focus on the interfaced layer, i.e. insulation layers next to the exterior and interior. The section in insulation material which shows the highest moisture content is then further simulated for mould growth risk, and compared to the laboratory mould growth test result.

2.3.1. Heat, air and moisture (HAM) simulation

For the HAM simulations, one-dimensional non-steady heat and moisture transport processes are solved by coupled differential equations using the software WUFI Pro [27], i.e. heat transport and moisture transport by.

$$\frac{\partial H}{\partial T}\frac{\partial T}{\partial t} = \frac{\partial}{\partial x}\left[\lambda\frac{\partial T}{\partial x}\right] + h_v\frac{\partial}{\partial x}\left[\frac{\delta}{\mu}\frac{\partial p}{\partial x}\right] \quad (4)$$

and.

$$\rho_w\frac{\partial w}{\partial \varphi}\bullet\frac{\partial \varphi}{\partial t} = \frac{\partial}{\partial x}\left[\rho_w D_w\frac{\partial w}{\partial \varphi}\frac{\partial \varphi}{\partial x}\right] + \frac{\partial}{\partial x}\left[\frac{\delta}{\mu}\frac{\partial p}{\partial x}\right] \quad (5)$$

respectively, where D_w ($m^2{\cdot}s^{-1}$) is the liquid transport coefficient, H

($J{\cdot}m^{-3}$) the enthalpy, h_v ($J{\cdot}kg^{-1}$) the evaporation enthalpy of water, p (Pa) the water vapour partial pressure, w ($m^3{\cdot}m^{-3}$) the water content, δ ($kg{\cdot}m^{-1}{\cdot}s^{-1}{\cdot}Pa^{-1}$) the water vapour diffusion coefficient in air, T (°C) the temperature, λ ($W{\cdot}m^{-1}{\cdot}K^{-1}$) the thermal conductivity, μ (dimensionless) the vapour diffusion resistance factor, ρ_w ($kg{\cdot}m^{-3}$) the density of water, and ϕ (dimensionless) the relative humidity RH.

The left-hand side of both equations consists of the storage terms, while the transport terms are on the right-hand side. In this model, the heat storage consists of the heat capacity of the material, the heat transport includes both moisture-dependent thermal conductivity and vapour enthalpy flow, the moisture storage is directly linked to the sorption isotherm, and the moisture transport contains both the liquid transport and vapour diffusion terms.

The design of the assembly wall in this study is based on two common exterior walls found in cold climate zones, i.e. masonry wall [28] and timber frame wall [29] with an air cavity as shown in Fig. 3. For comparative study purposes, the insulation layer thicknesses are adjusted to achieve an overall R-value of 4.7 $K{\cdot}m^2{\cdot}W^{-1}$ as per the Dutch requirement for an exterior wall in a residential building [30], or equivalent to a U-value of 0.205 $W{\cdot}m^{-2}{\cdot}K^{-1}$. Cellulose insulation material is included in the HAM study as the reference material, due to its low embodied energy among other conventional building materials [14]. Material properties of Cellulose and other building components of a masonry wall and timber frame wall (Wood Fibre Board, Gypsum Board, Solid Brick) are listed in Table 1 and Fig. 4. For the masonry wall, 10 cm thick bricks are applied for both exterior and interior sides, with 1.3 cm thick wood-fibre board as exterior sheathing board, and a 4 cm air cavity with an arbitrary air change rate of 10 h^{-1} (between the 5 and 20 h^{-1} used in [31]). For the timber frame wall, 2 cm spruce wood is applied as exterior cladding, similarly to a 4 cm fully ventilated air cavity as the brick cavity, with a 1.3 cm thick wood fibre and gypsum board as exterior and interior sheathing boards respectively. Building components outward from the ventilated air layer are set up for their shielding of rain and radiation, and are disregarded from the U-value calculation.

Six locations in Europe that represent different climate zones have been selected for the hygrothermal analysis. Table 2 shows the annual weather summary in all six locations, while Fig. 5 shows the annual air temperature and relative humidity profile [32]. Climate Cfa is represented by Milan with a humid subtropical climate, Climate Cfb for Eindhoven with a temperate oceanic climate, Climate Cfc for Tórshav with a subpolar oceanic climate, Climate Dfa for Kherson with a hot-summer humid continental climate, Climate Dfb for Oslo with a warm-summer humid continental climate, and Climate Dfc for Sodankylä with subarctic climate. The wall is facing the main driving rain direction (Table 2) for the hygrothermal simulations in all cases. The interior climate is set as per ISO 13788 with humidity class 3 which represents a building with unknown occupancy [33], and a constant air temperature of 20 °C. The simulation is run for ten years or until hygrothermal equilibrium is reached, and results from the final year are extracted for further analysis.

Table 1
Material properties for solid brick, wood fibre board, gypsum board and cellulose [34].

	Solid Brick	Wood Fibreboard	Gypsum Board	Cellulose (reference)
Bulk Density ρ_{bulk}, dried ($kg{\cdot}m^{-3}$)	1900	300	732	55
Porosity (%)	0.24	0.8	0.72	0.93
Specific Heat Capacity C_p ($J{\cdot}kg^{-1}{\cdot}K^{-1}$)	850	1400	1384	2544
Thermal Conductivity λ ($W{\cdot}m^{-1}{\cdot}K^{-1}$)	0.6	0.05	0.1925	0.0357
Vapour Diffusion Resistance Factor μ (dimensionless)	10	12.5	6.8	2
Free Water Saturation w_{sat} (%)	10	50	48	898

2.3.2. *Mould growth test*

The tests of the growth of mould on the specimen are carried out as per European Assessment Document EAD 040005–00-1201 Annex B [35], where test samples are exposed to a high humidity environment (close to 100 % RH) for four weeks at a constant temperature of 20 °C, by means of a desiccator with a bottom filled with water. After four weeks the specimen are visually inspected with the naked eye and microscope

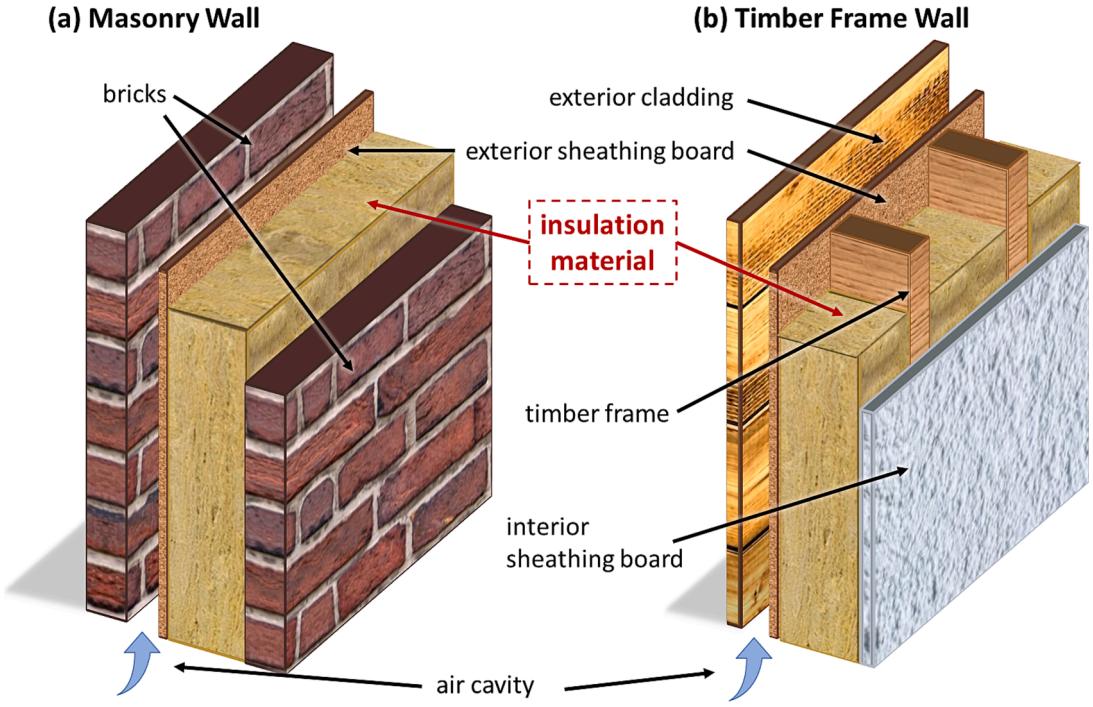

Fig. 3. Simulated wall assemblies (a) brick wall and (b) timber frame wall with air cavity.

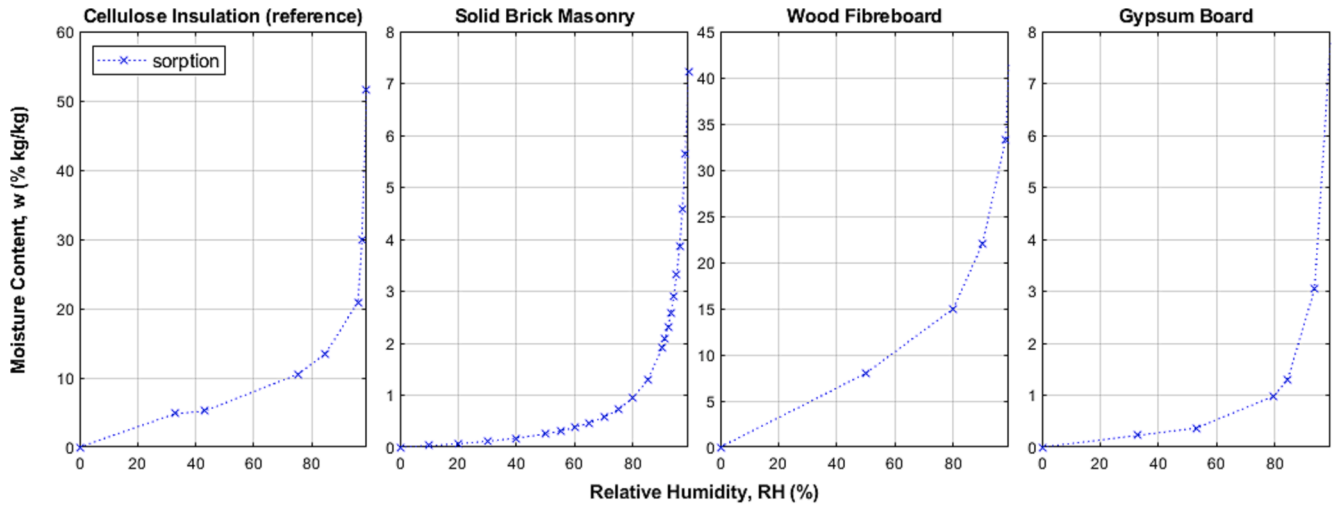

Fig. 4. Sorption curve for solid brick, wood fibreboard, gypsum board and cellulose [34]. Moisture content w after 99% RH is excluded from the plot for clarity, refer to w_{sat} for 100% relative humidity in Table 1.

Table 2
Summary of weather profile for simulated exterior climates.

Climate profile (Köppen climate classification)	Cfa	Cfb	Cfc	Dfa	Dfb	Dfc
Location	Milan, ITA	Eindhoven, NLD	Tórshav, FRO	Kherson, UKR	Oslo, NOR	Sodankylä, FIN
Altitude (m)	103	22	61	54	96	183
Temperature, mean (°C)	14.6	10.9	7.1	11.5	7.2	1.3
Relative Humidity, mean (%)	72.6	79.5	82.7	73.4	72.8	79.4
Wind Speed, mean ($m \cdot s^{-1}$)	1.8	3.8	6.6	2.9	2.7	2.6
Normal Rain, sum ($mm \cdot a^{-1}$)	754.5	733.7	1419.8	625.2	658.4	567.3
Counter Radiation, sum ($kWh \cdot m^{-2} \cdot a^{-1}$)	2978.9	2883.8	2715.3	2868.2	2661.8	2454.7
Driving Rain Direction, main (-)	NE	SW	West	NW	NE	SE

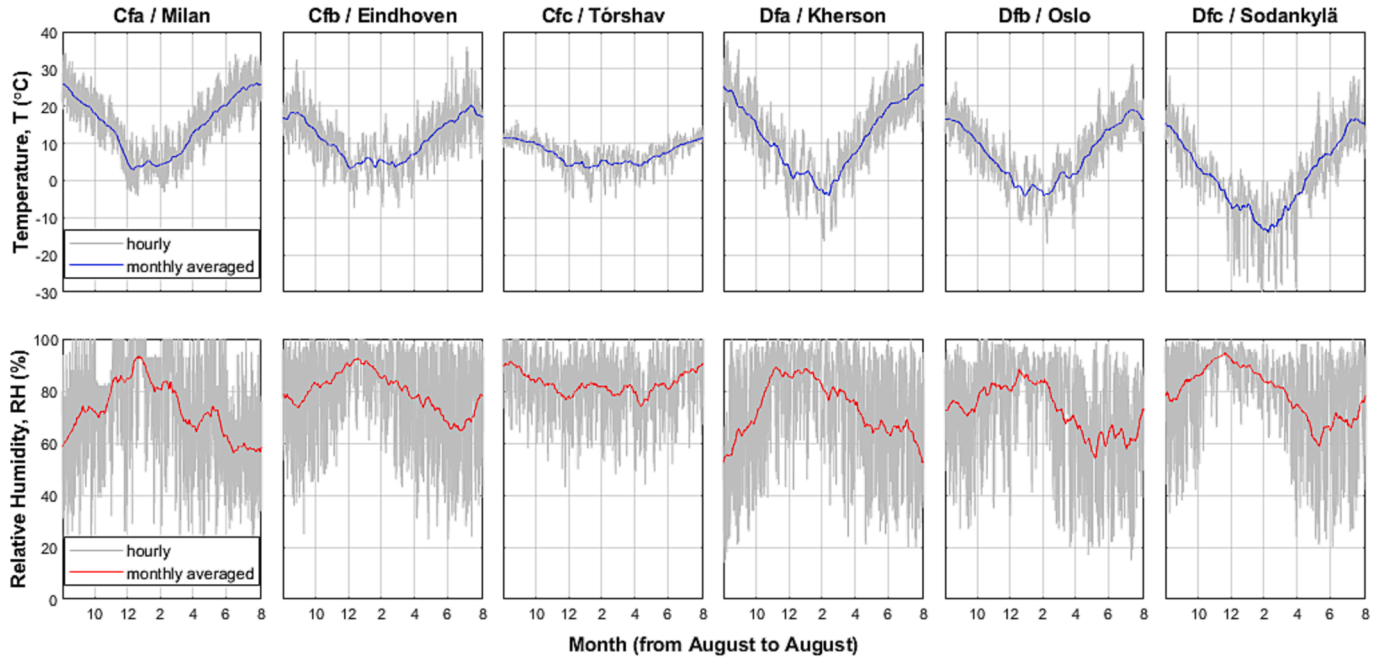

Fig. 5. Simulated Climates with Temperature and Relative Humidity profiles plotted against Months. Note Köppen climate classification description: C – temperate, D – continental, f – no dry season, a – hot summer, b – warm summer, c – cold summer.

(ZEISS Axio Imager 2) for the presence of mould fungus according to ISO 846 [36].

2.3.3. *Mould growth simulation*

The wall assemblies are further investigated in terms of mould growth risk under the chosen climates using the software WUFI Bio, based on the bio-hygrothermal model developed by Sedbauer et al. [37].

By using germination isopleth, i.e. the times needed for germination plotted in a temperature-humidity diagram and modelling the critical water content of potential mould spores, germination and mould growth can be predicted if water content in the model spore exceeds the critical water content. All samples in this study are assumed to be substrate class I, i.e. bio-utilizable substrates. This bio-hygrothermal model does not consider the biogenic factors, pH value, surface quality and several other influential factors that will impede germination and growth [38], therefore the simulation results obtained are rather conservative (higher mould growth risk) than in real conditions. It is therefore the simulation results are assessed in conjunction with the aforementioned laboratory mould growth test result.

3. Results and discussion

3.1. Thermal and hygric properties

3.1.1. Bulk density and porosity

All four studied insulation samples are of low bulk density and high porosity as shown in Table 3. The grass and hemp composites mainly consist of loose but interwoven cellulose fibres with open porosity, showing similar porosity at 96.5 % and 96.3 % respectively. For the mycelium composite, the fibres (mixture of straw, miscanthus and flax) are enveloped by the mycelium ligaments and have a denser and homogeneity coverage on the surface, and macroporous structures following the fibre packing remain inside the block, with porosity at 94.4 %. The cork composite has the lowest porosity at 87.4 % and contains both closed and open pores, where closed pore structures originated from their stacked hexagonal cells microstructure [39], and macro open pores formed during the expanded cork manufacturing process.

3.1.2. Sorption isotherms

The hemp, grass and mycelium composites show hydrophilic behaviour and have similar adsorption–desorption curves as shown in Fig. 6, and can absorb up to eight or nine times their weight of water under the full water immersion test (Table 3). The cork composite conversely has lower adsorption even with its porous structures, contributed by the hydrophobic nature of the surface of cork with a low wettability to water. It should be noted that the mycelium specimen (all three samples) under 98 % RH reached the maximum mass gain around the seventh day in the sorption test, and after that underwent mass loss and showed signs of mould growth on the surface. As a result, maximum mass gain instead of equilibrium mass is used to calculate the equilibrium moisture content at 98 % RH as shown in Fig. 6. The equilibrium moisture content under the desorption process is only slightly higher than the adsorption process, and no significant variation between both curves for all samples.

3.1.3. Water vapour diffusion resistance factor

The water permeability of the specimen is listed in Table 3. The hemp, grass and mycelium composites have a similar μ-factor around 3 under both dry and wet cup methods, and lower permeability at 10 (dry cup) and 14 (wet cup) for the cork composite.

Table 3
Density, Porosity, Specific Heat Capacity, Water Vapour Resistance Factor and Free Water Saturation for mycelium, hemp, grass and cork composites.

	Mycelium	Hemp	Grass	Cork
Bulk Density ρ_{bulk}, dried ($kg{\cdot}m^{-3}$)	97.1	64.1	60.1	97.9
Particle Density $\rho_{partocle}$ ($kg{\cdot}m^{-3}$)	1732.1	1747.3	1737.6	778.4
Porosity (%)	94.4	96.3	96.5	87.4
Specific Heat Capacity C_p ($J{\cdot}kg^{-1}{\cdot}K^{-1}$) at 20 °C	1167	1140	1110	1160
Water Vapour Resistance Factor μ				
-"Dry cup" condition (dimensionless)	3.4	3.0	2.9	9.7
-"Wet cup" condition (dimensionless)	3.2	2.6	2.6	13.9
Free Water Saturation w_{sat} (%)	816 %	889 %	910 %	117 %

3.1.4. Thermal conductivity

Fig. 7 summarizes the moisture-dependent thermal conductivity for all samples acclimatised to 0 %, 50 % and 80 % RH, showing the increase of thermal conductivity with higher RH except for the cork composite, which can be attributed to its hydrophobic surface. Though a generally linear relationship between thermal conductivity and moisture content of organic insulation materials is generally not holding, a simple linear fitting is nonetheless included in this study as input for subsequent hygrothermal simulation. In addition, uncertainties of 0.002 to 0.003 $W{\cdot}m^{-1}{\cdot}K^{-1}$ are presented in the measured thermal conductivities using the thermal needle probe. Under the steady-state condition, the grass composite has the lowest thermal conductivity 0.045 ± 0.003 $W{\cdot}m^{-1}{\cdot}K^{-1}$ at 0 % RH, and the cork composite exhibit an overall better thermal conductivity characteristic with a uniform 0.046 ± 0.003 $W{\cdot}m^{-1}{\cdot}K^{-1}$ under different RH. This is followed by the hemp and mycelium composite at 0.050 ± 0.004 and 0.051 ± 0.004 $W{\cdot}m^{-1}{\cdot}K^{-1}$ respectively. It should be noted that the declared thermal conductivity from the manufacturer of cork, grass and hemp composites is lower than the measurements in this study, i.e. 0.039, 0.040 and 0.040 $W{\cdot}m^{-1}{\cdot}K^{-1}$ respectively. The measured thermal conductivies are close to or in the range of other reported measurements, i.e. 0.037 to 0.041 $W{\cdot}m^{-1}{\cdot}K^{-1}$ for cork composite [15], 0.034 to 0.09 $W{\cdot}m^{-1}{\cdot}K^{-1}$ for grass composite [18], 0.038 and 0.06 $W{\cdot}m^{-1}{\cdot}K^{-1}$ for hemp composite [4], and 0.0404 to 0.0578 $W{\cdot}m^{-1}{\cdot}K^{-1}$ for mycelium composite [22].

3.1.5. Specific heat capacity

The specific heat capacity c_p of all four samples is in the range of 1100 to 1200 $J{\cdot}kg^{-1}{\cdot}°C^{-1}$ as listed in Table 3 and Fig. 8.

3.1.6. Thermal stability

Thermogravimetric analysis of the samples is shown in Fig. 9. All four samples are thermally stable up to about 200 °C, and thereafter start to decompose and reach their maximum rate of weight loss between 300 and 350 °C. It is, therefore, necessary to protect these insulation composites from fire hazards with other fire and heat resistant components, e.g. bricks, sheathing boards, etc.

The decomposition process of the samples follows a similar trend, corresponding to hemicelluloses being pyrolyzed in the range of 200 and 300 °C, depolymerized cellulose in the range of 300 and 350 °C, lignin components pyrolyzed in the range of 225 and 450 °C [40]. For cork composite, depolymerization of suberin appears between 400 and 500 °C [41]. The second peak at 400 °C is also observed on the grass composite, contributed by other recycled materials mixed in the composite. Likewise, a similar small peak can be noticed for the hemp composite where recycled materials are also used. All composites end their volatile emissions at around 450 °C with a remaining char residue of around 20 to 30 % of the original dry weight.

3.2. HAM simulations

3.2.1. Thermal transmittance

Based on the thermal conductivity findings in Fig. 7, the insulation thickness for both wall types (Fig. 3) and all four studied insulation materials are formulated to achieve an overall R-value of 4.7 $K{\cdot}m^2{\cdot}W^{-1}$ as per the Dutch requirement for an exterior wall in a residential building [30], or equivalent to a U-value of 0.205 $W{\cdot}m^{-2}{\cdot}K^{-1}$. The thicknesses are listed in Table 4, and it can be seen that all four materials require a higher wall thickness in comparison to reference Cellulose insulation material.

The transient thermal transmittance U-value of the investigated insulation materials under two different wall types and six different climates are investigated and summarized in Fig. 10. Only transient U-values in the 'heating period' from October to March are included as the

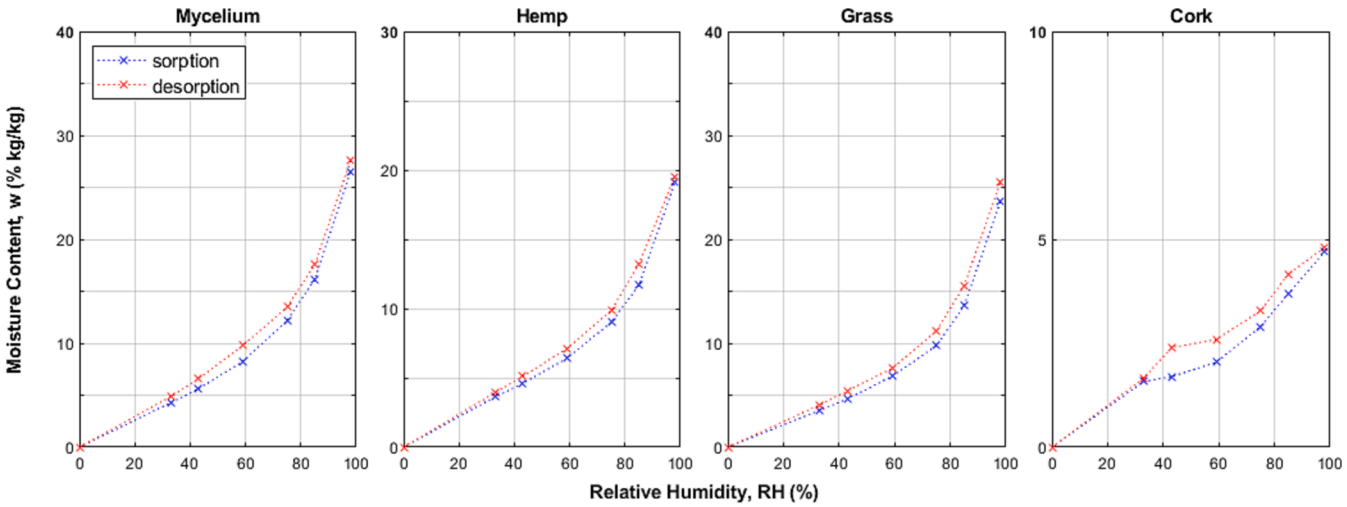

Fig. 6. Sorption-desorption curves with Moisture Content w plotted against RH for mycelium, hemp, grass and cork composites. For Moisture Content at 100% RH, refer to w_{sat} in Table 3.

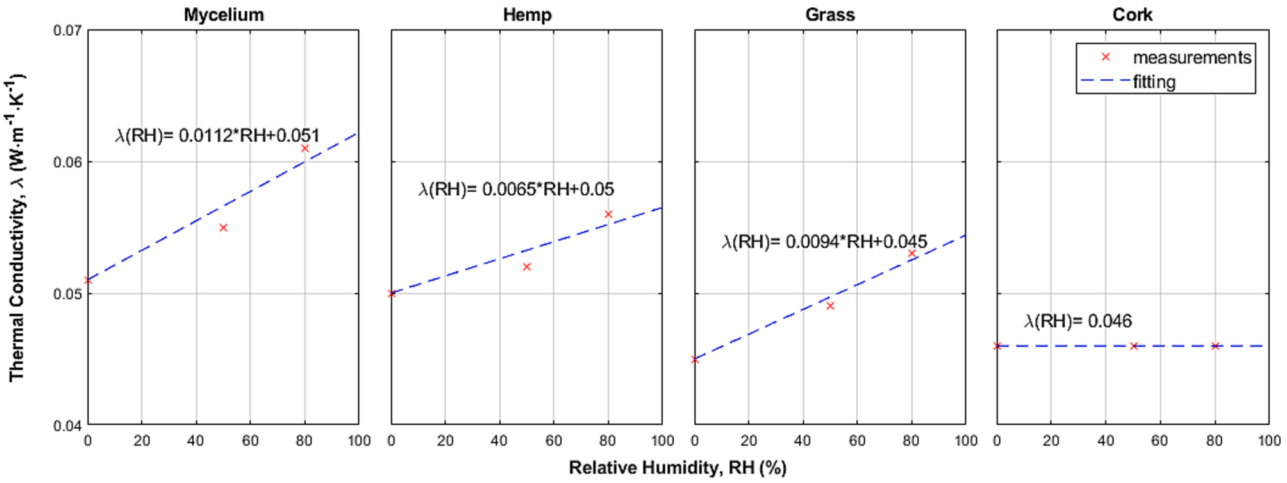

Fig. 7. Thermal Conductivity λ against RH for mycelium, hemp, grass and cork composites.

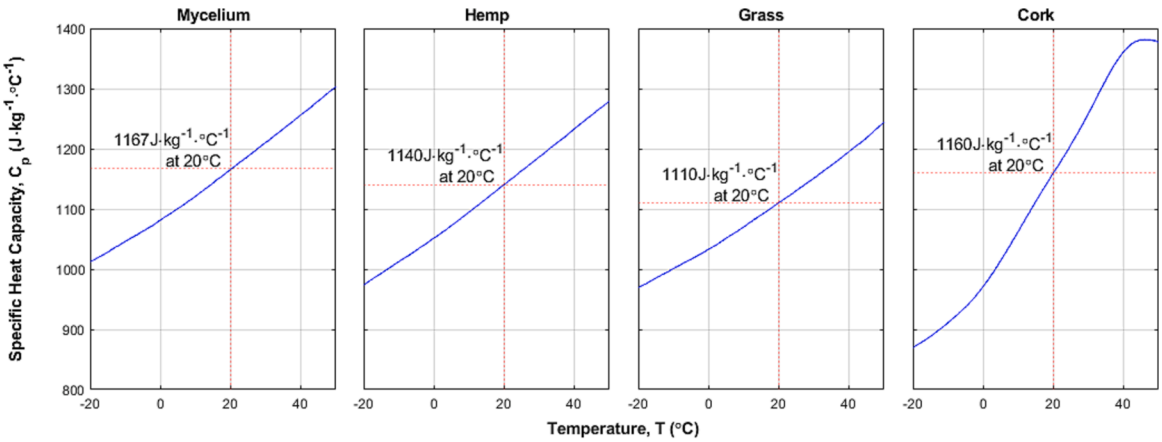

Fig. 8. Specific heat capacity C_p against Temperature T for mycelium, hemp, grass and cork composites.

U-value under warmer months will yield non-sensible results and is not of interest in this study.

In general, all four insulation materials display matching trends of transient U-value under a combination of the same climate and wall type, however, diverge significantly when compared across different climates or wall types of the same material. Under continental climate Dfa (Kherson), Dfb (Oslo) and Dfc (Sodanskylä), the insulated walls provide uniform thermal insulation performance close to the designed

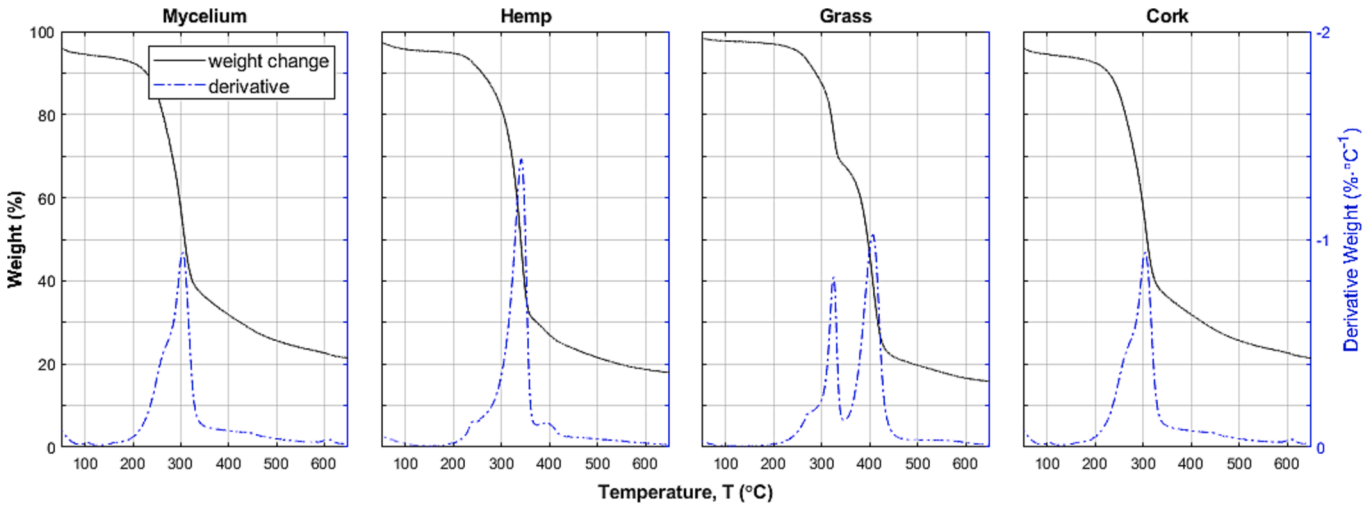

Fig. 9. Thermal stability against temperature T for mycelium, hemp, grass and cork composites.

Table 4
Insulation thickness and total wall thickness (in bracket) for simulation.

	Mycelium	Hemp	Grass	Cork	Cellulose (reference)
Brick Wall (mm)	209.5 (463)	202.6 (456)	184.6 (438)	184.8 (438)	160.6 (414)
Timber Frame Wall (mm)	209.3 (295)	202.4 (288)	184.4 (270)	184.7 (271)	160.5 (247)

U-value at 0.205 $W \cdot m^{-2} \cdot K^{-1}$ in the heating period. Higher transient U-values however are observed on the walls under temperate climates Cfa (Milan), Cfb (Eindhoven) and Cfc (Tórshav), coincide with their milder and wetter climate profiles. On the whole, the insulated timber frame walls perform better than the brick walls, in particular under temperature climates, when a similar initial designed U-value is set for all cases. This is a consequence of the thicker and denser brick layers (Table 1) which hamper the moisture transport in the wall assemblies, causing higher moisture accumulation in the insulation material (Section 3.2.2). This pattern reaffirms the central role of exterior climates and type of

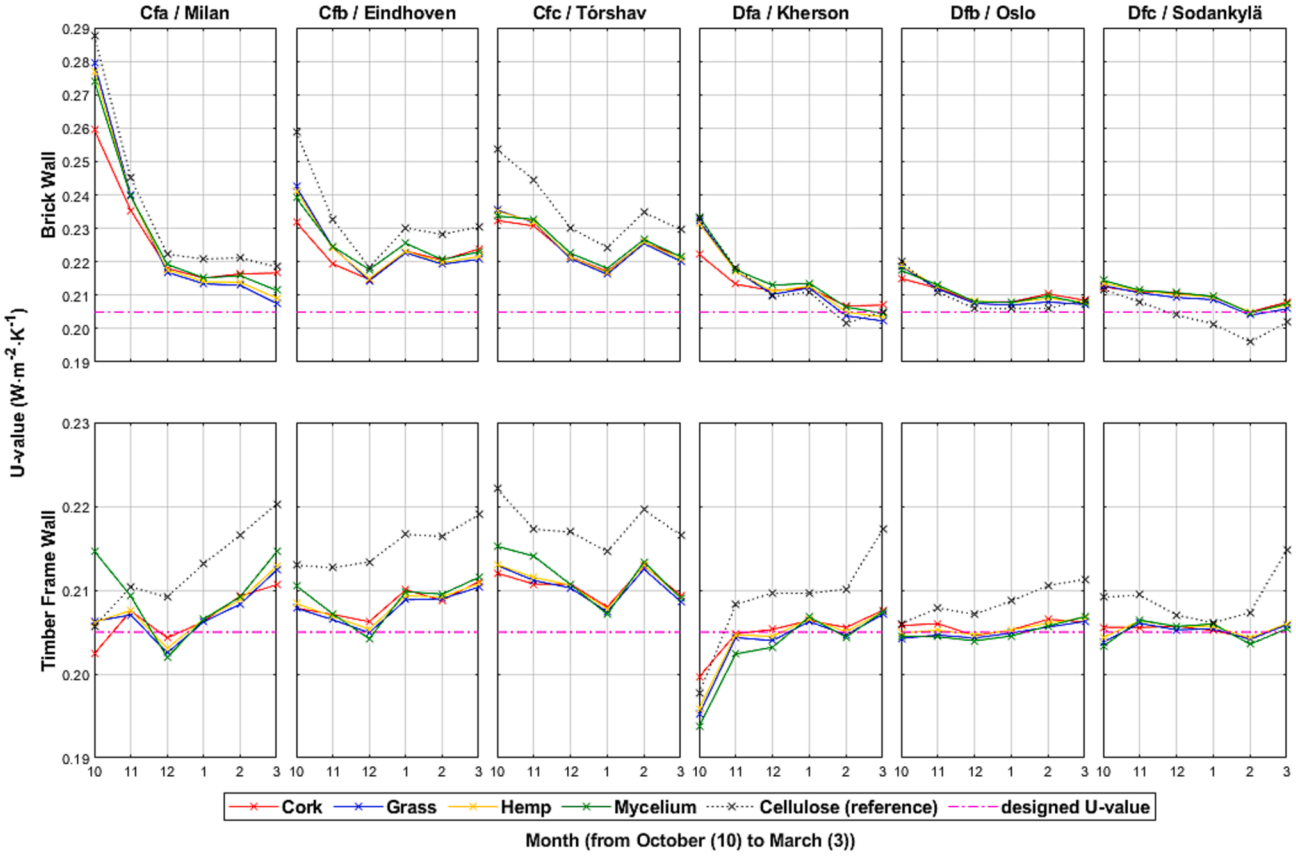

Fig. 10. Transient thermal transmittance (U-value) for mycelium, hemp, grass and cork composites in heating period (October to March) under different Wall Assemblies Types and Climates/Locations.

building envelop design in the evaluation of building insulation performance, when a similar category of insulation materials are to be considered, in this case, the bio-based insulation materials.

If without considering durability aspects from potential deterioration due to mould growth under a humid environment, or no concern of overall wall thickness owing to the thickness of insulation layer required for the intended U-value, there is no specific material to be recommended based on their transient U-value performance. However, when the wall thickness is of interest, the cork composite with its less demanding thickness requirement is the preferred selection compared to other investigated bio-based materials, followed by the grass composites.

3.2.2. Moisture content

The equilibrium moisture content in the investigated bio-based insulation composites under two different wall types and six different climates in a simulated year is shown in Fig. 11. Mycelium composite shows the highest moisture content under all climates and wall types, while cork composite shows the lowest and the most regulated moisture content throughout the year in general. Both grass and hemp composites exhibit similar moisture content to the reference cellulose insulation material. These dynamic moisture content of the composites are in agreement with their sorption isotherm, i.e. higher sorption capacity of mycelium composite and the opposite for cork composite (Fig. 6).

Higher moisture content in an insulation layer can be found at the near-interfaced layers, in the case of the selected wall type and climates, they are either at layers next to the exterior sheathing board or behind the interior sheathing board. The moisture content of both interfaced layers in a simulated year is extracted and presented in Fig. 12. A few observations can be generalized based on the climate types: for Cfa (Milan) and Dfa (Kherson), moisture tends to accumulate at the exterior interface during the winter period and interior interface during the summer period; for Cfb (Eindhoven), Dfb (Oslo) and Dfc (Sodanskylä), moisture accumulation is generally found on the exterior interface during the winter period, and while the moisture content is increasing on the interior interface during summertime it is still not exceeding that of the exterior side; and for Cfc (Tórshav), the moisture content at the exterior interface is always higher than the interior interface. It can be established that the insulation layer at the exterior interface has the highest averaged moisture content under all six climates, and consequently is most likely subjected to mould growth and degradation compared to other parts of insulation under different climate conditions.

In terms of wall type, insulation material inside the timber frame walls have generally lower moisture content at the exterior interface than those inside brick walls across different climates except Dfc (Sodanskylä). The opposite trend is observed at the interior interface where the insulation layer in timber frame walls has higher moisture content compared to brick walls. Note that no vapour retarder is included in the design of all simulated walls to retard the vapour diffusion process, and a ventilated air cavity is included in all cases to provide additional hygrothermal regulation to the overall wall assembly.

3.3. Mould growth risk

3.3.1. Mould growth test

After exposing the test specimen for four weeks to high humidity in a desiccator filled with water, the specimen is visually inspected with the naked eye and microscope for the presence of mould. Fig. 13 shows photos taken on the specimen with and without high humidity conditioning. The fungal growth on the test specimen is assessed according to ISO 846 [36] and the intensity scales of mould growth are assigned to them in Table 5.

Significant mould growth and degradation are found on the

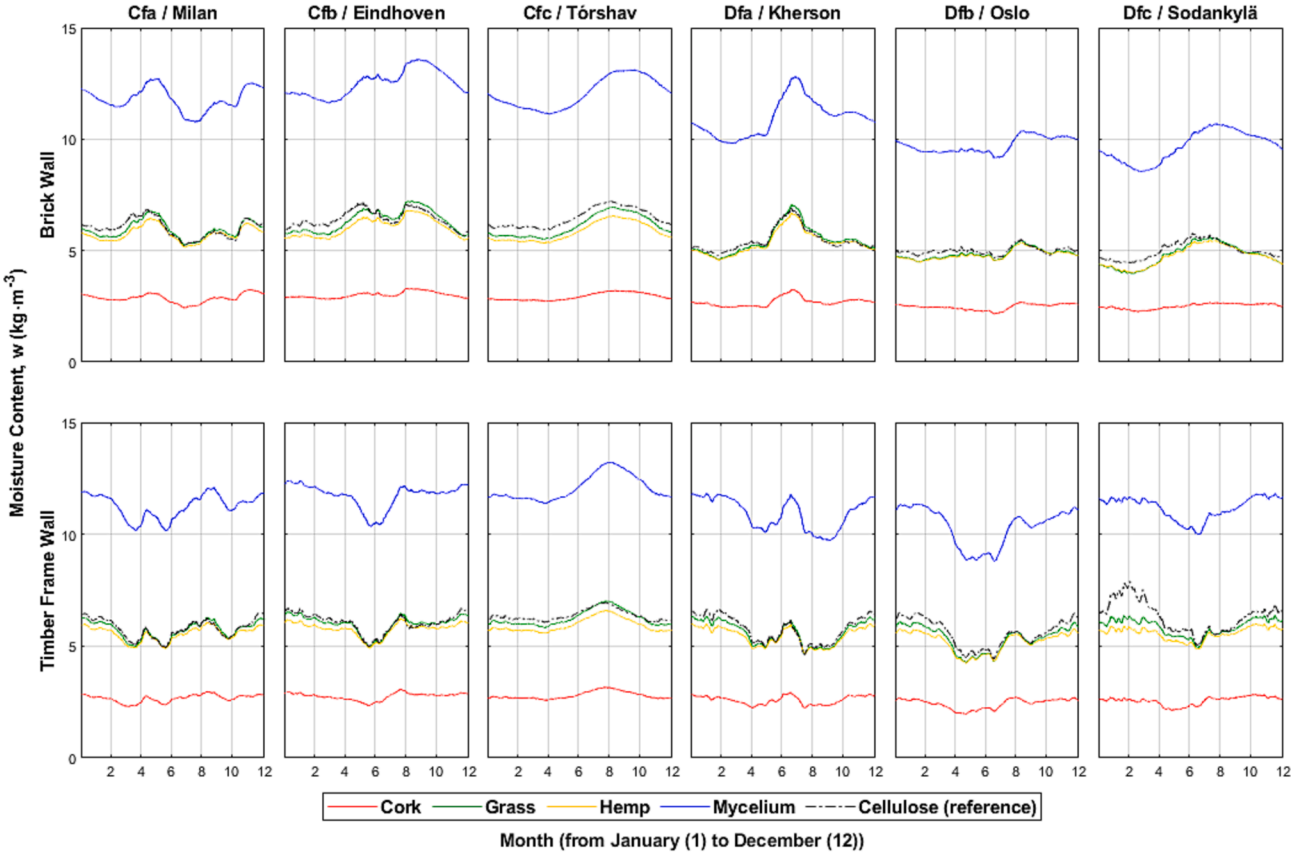

Fig. 11. Moisture Content w for mycelium, hemp, grass and cork composites under different Wall Assemblies Types, Climates/Locations and Months.

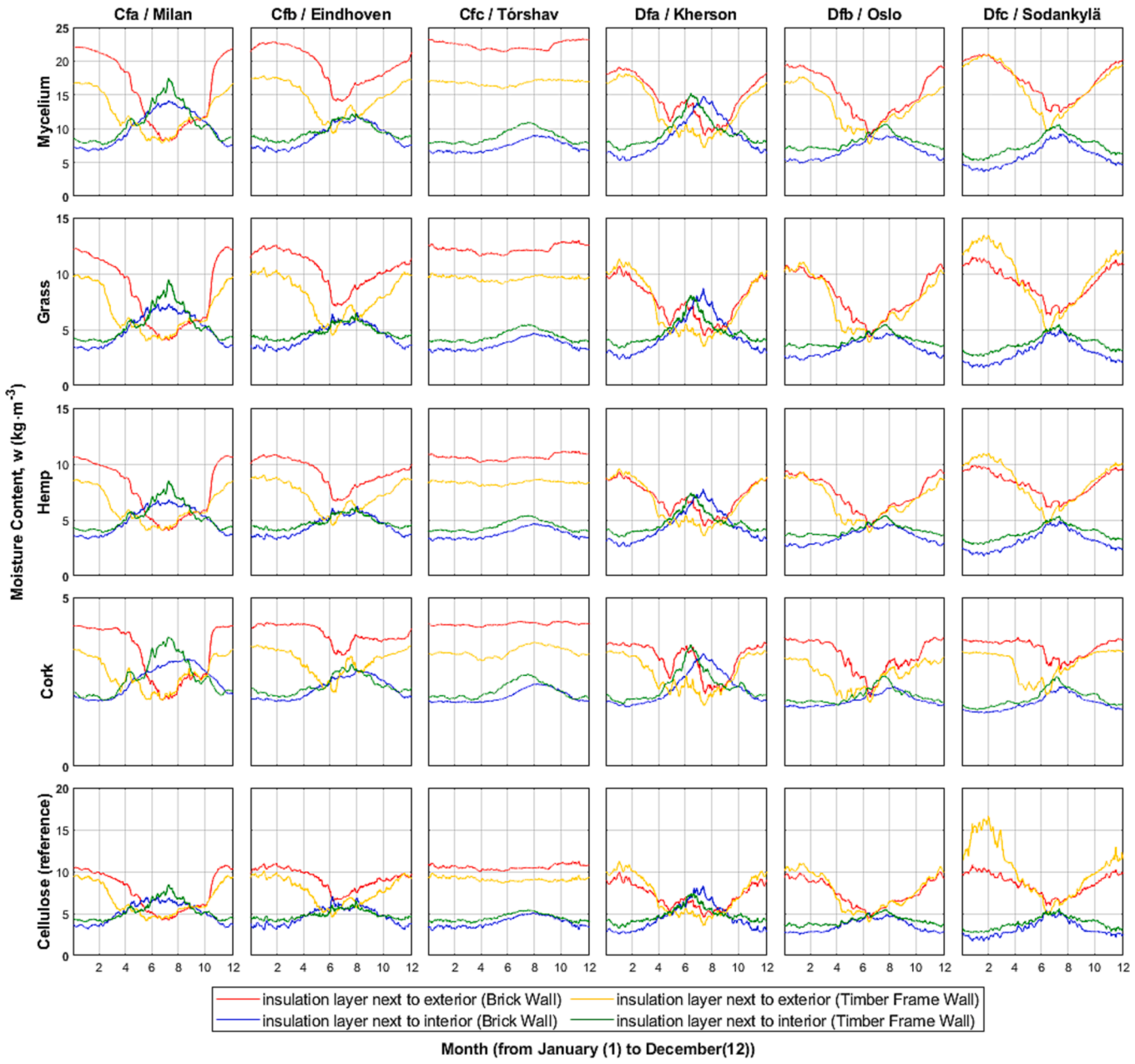

Fig. 12. Moisture Content w at insulation layer next to the exterior and next to interior under different Wall Assemblies Types, Climates/Locations and Months.

mycelium composite. Note that mould growth was already observed on mycelium composite conditioned under 98 % RH in the sorption test, as discussed in section 3.1. Discolouring on the hemp composite can be perceived with naked eyes and fungi are distinguished easily under a microscope. For the grass composite, no obvious mould growth or discolouring is observed with the naked eye, however, deterioration of the fibres is noticeable under the microscope. No apparent deterioration, mould growth or discolouring is detected on the cork composite. These results are in agreement with the literature: similar mould development can be distinguished with the naked eye on the mycelium-miscanthus test sample by Dias et al. (2021) [21]; fungi contamination can be observed under a microscope on hemp shiv composites by Viel et al. (2019) [42]; on the other hand mould development on grass and cork composite is not presented on the literature.

3.3.2. *Mould growth simulation*

The mould growth risk of the wall assemblies under the chosen climates is further simulated, and the results are shown in Fig. 14. The insulation layer made of any of the four composites under temperate climates Cfa, Cfb and Cfc in masonry walls are predicted with heavy mould growth with a mould index above 3. For timber frame walls, a high mould index is predicted for the mycelium, hemp and grass composites only under Cfc climate, and medium mould growth potential for the grass composite under Cfb climate. Under continental climate Dfa, Dfb and Dfc, low mould growth potential is predicted for both wall designs and all four composites. Overall, lower mould growth risk is predicted for timber frame walls in comparison to brick walls.

4. Conclusions and recommendations

4.1. *Conclusions*

This research examines the thermal and hygric characteristics of the selected bio-based composites, namely mycelium, hemp, grass and cork

Fig. 13. Mould evaluation test (1) mycelium, (2) hemp, (3) grass and (4) cork composites. For subset, (a) and (c) are samples without conditioning, (b) and (d) are samples conditioned under high RH.

Table 5
Assessment of mould growth.

Composites	Intensity of growth	Evaluation
Mycelium	5	Heavy growth, covering the entire test surface
Hemp	3	Growth visible to the naked eye, covering up to 50 % of the test surface
Grass	1	No growth is visible to the naked eye, but visible under the microscope
Cork	0	No growth is apparent under the microscope

composites, and simulates their hygrothermal performances with two construction details and six different climates in Europe.

Among all four investigated composites, cork composite exhibit the lowest thermal conductivity, low sorption properties and no mould growth risk. The hemp, grass and mycelium composites have similar hygric properties and show deterioration under mould growth test in the lab. Mycelium composite has the worst examined characteristics and performance, with the highest thermal conductivity and is vulnerable to mould growth in a humid environment.

In actual building applications, exterior climates and wall designs are the main factors in determining the hygrothermal performances of insulation material. It is found that the simulated timber frame wall with a fully ventilated cavity is more suitable for low-density bio-based insulation materials when compared to a fully ventilated brick wall, and the mould growth potential of the studied insulation materials is higher under temperate climates Cfa, Cfb and Cfc when compared to continental climates Dfa, Dfb and Dfc.

The findings in this study underline the suitability of using different bio-based composites according to the assembly design and the local climate conditions and provide a guideline in choosing the correct insulation material under different geometry of the enclosure and boundary conditions.

4.2. Recommendations

By combining the mould growth laboratory testing and the hygrothermal simulation results, the following are the recommendations if the studied bio-based composites are to be applied as a thermal insulation material:

a. Mycelium composite is not recommended under temperate climates Cfa, Cfb and Cfc. It is also not recommended in any built environment with high humidity conditions (>80 % RH) due to its susceptibility to

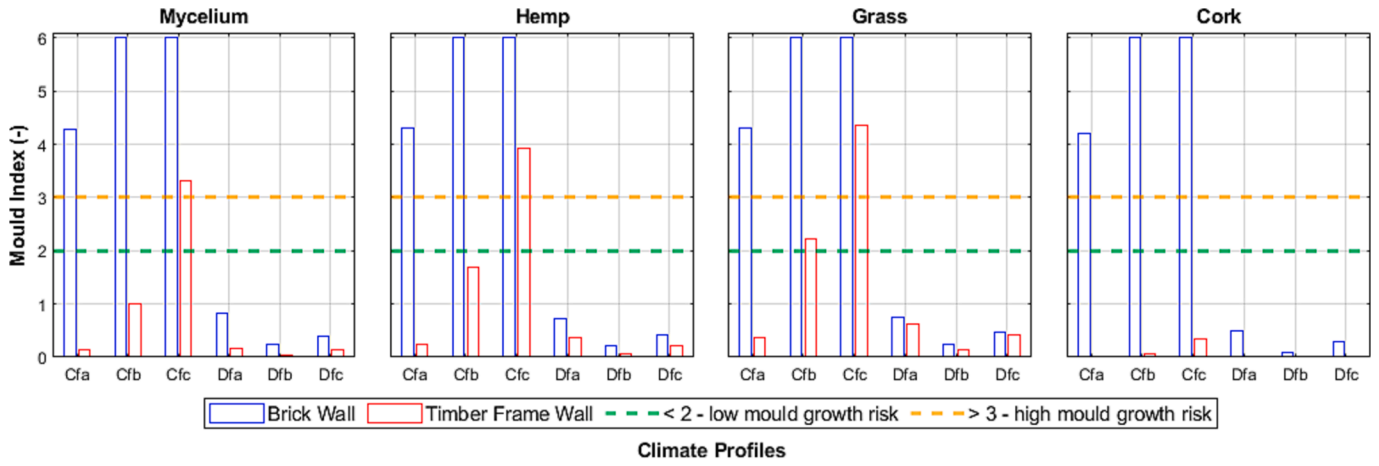

Fig. 14. Predicted Mould Index for mycelium, hemp, grass and cork composites under different Wall Assemblies Types and Climates/Locations.

rapid mould growth. Airtightness of wall construction is necessary to avoid direct water exposure or high humidity condition.

b. Hemp and grass composites are not recommended under temperate climates Cfa, Cfb and Cfc. Airtightness of wall construction is necessary to avoid direct water exposure or high humidity condition.
c. Cork composite is suitable under the investigated temperate and continental climates, either as exposed or covered components.
d. Timber frame wall is more suitable for low-density bio-based insulation material when compared to brick walls

CRediT authorship contribution statement

C.H. Koh: Conceptualization, Methodology, Investigation, Formal analysis, Writing – original draft. **F. Gauvin:** Writing – review & editing, Supervision. **K. Schollbach:** Writing – review & editing, Supervision. **H. J.H. Brouwers:** Writing – review & editing, Supervision.

Declaration of Competing Interest

The authors declare that they have no known competing financial interests or personal relationships that could have appeared to influence the work reported in this paper.

Data availability

Data will be made available on request.

References

[1] United Nations Environment Programme, "2021 Global Status Report for Buildings and Construction: Towards a Zero–emission, Efficient and Resilient Buildings and Construction Sector.," Nairobi, 2021.
[2] GlobalABC/IEA/UNEP (Global Alliance for Buildings and Construction, International Energy Agency, and the United Nations Environment Programme) , "GlobalABC Roadmap for Buildings and Construction: Towards a zero-emission, efficient and resilient buildings and construction sector," IEA, Paris, 2020.
[3] D. Jones, "1.2 Bio-based building materials and their role in the modern building sector," in *Performance of Bio-based Building Materials*, Woodhead Publishing, 2017, pp. 2-4. doi: 10.1016/B978-0-08-100982-6.00001-X.
[4] G. Grazieschi, F. Asdrubal, G. Thomas, Embodied energy and carbon of building insulating materials: a critical review, Clean. Environ. Syst. 2 (2021), 100032, https://doi.org/10.1016/j.cesys.2021.100032.
[5] C.C. Pavel, D.T. Blagoeva, Competitive landscape of the EU's insulation materials industry for energy-efficient buildings, Publications Office of the European Union, Luxembourg, 2018.
[6] C. Brischke, "5.4 Moisture performance," in *Performance of Bio-based Building Materials*, Woodhead Publishing, 2017, pp. 277-285. doi:10.1016/B978-0-08-100982-6.00005-7.
[7] J. V. Acker and S. Palanti, "5.3 Durability," in *Performance of Bio-based Building Materials*, Woodhead Publishing, 2017, pp. 257-277. doi:10.1016/B978-0-08-100982-6.00005-7.
[8] C.P. Hoang, K.A. Kinney, R.L. Corsi, P.J. Szaniszlo, Resistance of green building materials to fungal growth, Int. Biodeterior. Biodegrad. 64 (2) (2010) 104–113, https://doi.org/10.1016/j.ibiod.2009.11.001.
[9] A. Brambilla, A. Sangiorgio, Mould growth in energy efficient buildings: causes, health implications and strategies to mitigate the risk, Renew. Sustain. Energy Rev. 132 (2020), 110093, https://doi.org/10.1016/j.rser.2020.110093.
[10] GRAMITHERM, "Gramitherm," [Online]. Available: https://gramitherm.ch/products/?lang=en. [Accessed 25 3 2022].
[11] "HEMPFLAX," [Online]. Available: https://www.hempflax.com/en/applications/construction/. [Accessed 25 3 2022].
[12] FAIRM, "FAIRM foam," [Online]. Available: https://www.fairm.nl/material. [Accessed 25 3 2022].
[13] "PROSUBER," [Online]. Available: https://www.prosuber.com/geexpandeerde-kurk-productinformatie/. [Accessed 25 3 2022].
[14] D. Kumar, M. Alam, P.X. Zou, J.G. Sanjayan, R.A. Memon, Comparative analysis of building insulation material properties and performance, Renew. Sustain. Energy Rev. 131 (2020), 110038, https://doi.org/10.1016/j.rser.2020.110038.
[15] E. Elsacker, S. Vandelook, J. Brancart, E. Peeters, L. De Laet, D. Aydemir, Mechanical, physical and chemical characterisation of mycelium-based composites with different types of lignocellulosic substrates, PLoS ONE 14 (7) (2019), https://doi.org/10.1371/journal.pone.0213954.
[16] N. Simões, R. Fino, A. Tadeu, Uncoated medium density expanded cork boards for building façades and roofs: mechanical, hygrothermal and durability characterization, Constr. Build. Mater. 200 (2019) 447–464, https://doi.org/10.1016/j.conbuildmat.2018.12.116.
[17] R. Fino, A. Tadeu, N. Simões, Influence of a period of wet weather on the heat transfer across a wall covered with uncoated medium density expanded cork, Energy Build. 165 (2018) 118–131, https://doi.org/10.1016/j.enbuild.2018.01.020.
[18] A. Tadeu, L. Škerget, N. Simões, R. Fino, Simulation of heat and moisture flow through walls covered with uncoated medium density expanded cork, Build. Environ. 142 (2018) 195–210, https://doi.org/10.1016/j.buildenv.2018.06.009.
[19] T. Teppand, "3.9 Grass," in *Performance of Bio-based Building Materials*, Woodhead Publishing, 2017, pp. 150-156. doi:10.1016/B978-0-08-100982-6.00003-3.
[20] E. Latif, S. Tucker, M.A. Ciupala, D.C. Wijeyesekera, D. Newport, Hygric properties of hemp bio-insulations with differing compositions, Constr. Build. Mater. 66 (2014) 702–711, https://doi.org/10.1016/j.conbuildmat.2014.06.021.
[21] F. Collet, F. Achchaq, K. Djellab, L. Marmoret, H. Beji, Water vapor properties of two hemp wools manufactured with different treatments, Constr. Build. Mater. 25 (2) (2011) 1079–1085, https://doi.org/10.1016/j.conbuildmat.2010.06.069.
[22] P.P. Dias, L.B. Jayasinghe, D. Waldmann, Investigation of Mycelium-Miscanthus composites as building insulation material, Results Mater. 10 (2021), 100189, https://doi.org/10.1016/j.rinma.2021.100189.
[23] Z. Yang, F. Zhang, B. Still, M. White, Physical and mechanical properties of fungal mycelium-based biofoam, J. Mater. Civ. Eng. 29 (7) (2017) 04017030, https://doi.org/10.1061/(ASCE)MT.1943-5533.0001866.
[24] J.M.P.Q. Delgado, E. Barreira, N.M.M. Ramos, V.P.d. Freitas, Hygrothermal Numerical Simulation Tools Applied to Building Physics, SpringerBriefs, Comput. Mech. (2013), https://doi.org/10.1007/978-3-642-35003-0_1.
[25] ASTM, "ASTM C1498-01 Standard test method for hygroscopic sorption isotherms of building materials".
[26] ASTM, "ASTM E96-00 Standard test methods for water vapour transmission of materials".
[27] WUFI, "WUFI Pro 6.4 online help, Appendix: Basic: moisture transport in building materials".
[28] SINTEF Community, "Byggdetaljer 523.231 Skallmurvegger," in *Byggforskserien*, SINTEF, 2020.
[29] SINTEF Community, "Byggdetaljer 523.255 Yttervegger av bindingsverk. Varmeisolering og tetting," in *Byggforskserien*, SINTEF, 2020.
[30] Bouwbesluit 2012, "Hoofdstuk 5. Technische bouwvoorschriften uit het oogpunt van energiezuinigheid en milieu. Artikel 5.3. Thermische isolatie".

[31] M. Salonvarra, A. Karagiozis, M. Pazera and W. Miller, "Air Cavities Behind Claddings - What Have We Learned?," 1995.
[32] Dru Crawley; Linda Lawrie, "Climate.OneBuilding.Org," [Online]. Available: https://climate.onebuilding.org/default.html. [Accessed 25 3 2022].
[33] ISO, "ISO 13788 Hygrothermal performance of building components and building elements - internal surface temperature to avoid critical surface humidity and interstitial condensation - calculation method," 2012.
[34] WUFI, Wufi Material, Database 2022.
[35] Eota, "ead, Factory-made thermal and/or acoustic insulation products made of vegetable or animal fibres," EOTA 2015 040005–00-1201.
[36] ISO, "ISO 846 Plastics - evaluation of the action of microorganisms," 1997.
[37] K. Sedlbauer, M. Krus and K. Breuer, "Mould Growth Prediction with a New Biohygrothermal Method and its Application in Practice," in *Materials Conference*, Lodz, 2003.
[38] WUFI, *WUFI-Bio 40.0 Help: Limitations of the Model.*.
[39] H. Pereira and S. Knapic, "2.7 Bark and cork," in *Performance of Bio-based Building Materials*, Woodhead Publishing, 2017, pp. 78-86. doi:10.1016/B978-0-08-100982-6.00002-1.
[40] R. H. White and M. A. Dietenberger, "Fire Safety of Wood Construction: Thermal Degradation of Wood," in Wood Handbook, Madison, USDA, Forest Service, Forest Products Laboratory, 2010, pp. 18–8.
[41] A. Şen, J. Van den Bulcke, N. Defoirdt, J. Van Acker, H. Pereira, Thermal behaviour of cork and cork components, Thermochim. Acta 582 (2014) 94–100.
[42] M. Viel, F. Collet, Y. Lecieux, M.L.M. François, V. Colson, C. Lanos, A. Hussain, M. Lawrence, Resistance to mold development assessment of bio-based building materials, Compos. B Eng. 158 (2019) 406–418, https://doi.org/10.1016/j.compositesb.2018.09.063.